Spatial Variability of Shortwave Irradiance for Snowmelt in Forests

JOHN POMEROY,* ALED ROWLANDS,+ JANET HARDY,# TIM LINK,@ DANNY MARKS,&
RICHARD ESSERY,+ JEAN EMMANUEL SICART,** AND CHAD ELLIS*

* *Centre for Hydrology, University of Saskatchewan, Saskatoon, Saskatchewan, Canada*
+ *Institute of Geography and Earth Science, University of Wales, Aberystwyth, Ceredigion, United Kingdom*
# *U.S. Army Cold Regions Research and Engineering Laboratory, Hanover, New Hampshire*
@ *Department of Forest Resources, University of Idaho, Moscow, Idaho*
& *Northwest Watershed Research Center, Agricultural Research Service, USDA, Boise, Idaho*
** *Great Ice, Institut de Recherche pour le Développement, Montpellier, France*

(Manuscript received 4 January 2007, in final form 6 September 2007)

ABSTRACT

The spatial variation of melt energy can influence snow cover depletion rates and in turn be influenced by the spatial variability of shortwave irradiance to snow. The spatial variability of shortwave irradiance during melt under uniform and discontinuous evergreen canopies at a U.S. Rocky Mountains site was measured, analyzed, and then compared to observations from mountain and boreal forests in Canada. All observations used arrays of pyranometers randomly spaced under evergreen canopies of varying structure and latitude. The spatial variability of irradiance for both overcast and clear conditions declined dramatically, as the sample averaging interval increased from minutes to 1 day. At daily averaging intervals, there was little influence of cloudiness on the variability of subcanopy irradiance; instead, it was dominated by stand structure. The spatial variability of irradiance on daily intervals was higher for the discontinuous canopies, but it did not scale reliably with canopy sky view. The spatial variation in irradiance resulted in a coefficient of variation of melt energy of 0.23 for the set of U.S. and Canadian stands. This variability in melt energy smoothed the snow-covered area depletion curve in a distributed melt simulation, thereby lengthening the duration of melt by 20%. This is consistent with observed natural snow cover depletion curves and shows that variations in melt energy and snow accumulation can influence snow-covered area depletion under forest canopies.

1. Introduction

The ablation of snow cover in complex environments remains a difficult phenomenon to model because of the high variability of both snow water equivalent (SWE; snow mass per unit area expressed as a depth of equivalent water) and incident energy to snow. Fine-scale spatially distributed models have calculated SWE and ablation over complex open landscapes and shown realistic-looking snow cover depletion over areas up to a few square kilometers (Marks and Winstral 2001). The application of these computationally and parameter intensive small-scale models to large river basins or atmospheric model grid cells is not currently feasible; therefore, scaling relationships have been adopted that refer to the effects of the spatial variability of initial SWE and ablation energy on the snow-covered area during ablation.

Buttle and McDonnell (1987) noted that the areal rate of depletion of snow cover can be influenced by the spatial variation in SWE or ablation rate, or some combination of the two. At the unresolved "subtile" or "subgrid" scales, the depletion of snow cover has been calculated using an initial frequency distribution of snow water equivalent and the assumption of spatially invariant energy inputs (e.g., Shook et al. 1993; Donald et al. 1995; Brubaker and Menoes 2001), and using frequency distributions of both initial SWE and ablation energy (Faria et al. 2000; Pomeroy et al. 2001; Essery and Pomeroy 2004). The fractional snow-covered area (f_s) can be found from the joint probability distributions of point SWE and ablation energy (M; expressed as an equivalent mass loss) as

Corresponding author address: John Pomeroy, Centre for Hydrology, University of Saskatchewan, 117 Science Place, Saskatoon SK S7N5CB, Canada.
E-mail: john.pomeroy@usask.ca

DOI: 10.1175/2008JHM867.1

$$f_s = \int_M^\infty \int_{\text{SWE}}^\infty p(M, \text{SWE})\, dM\, d\text{SWE}, \qquad (1)$$

and the remaining areal mean SWE during melt can, similarly, be found as

$$\overline{\text{SWE}} = \int_M^\infty \int_{\text{SWE}}^\infty (\text{SWE} - M) p(M, \text{SWE})\, dM\, d\text{SWE}. \qquad (2)$$

The joint frequency distribution approach outlined by Eqs. (1) and (2) appears necessary in complex terrain and forested environments and is intractable to solve using analytical means (Faria et al. 2000; Essery and Pomeroy 2004). Shook (1995) showed that the frequency distribution of SWE can be matched to a lognormal distribution described by the mean and variance; therefore, much work has gone into examining the coefficient of variation (CV) of SWE and M in various environments and using these parameters and the lognormal frequency function to devise snow-covered area depletion algorithms (Pomeroy et al. 1998; Faria et al. 2000; Pomeroy et al. 2001; Pomeroy et al. 2004; Essery and Pomeroy 2004). Although the CV of SWE appears repeatable for many landscape types (Pomeroy et al. 1998), the processes influencing the CV of M are less clear.

The primary problem in calculating snow-covered area depletion using spatial distributions of ablation energy is that there is almost no information available on spatial distributions of the components of energy inputs to snow; hence, there is little physical basis on which to estimate the distributions of M. An important component of energy to melting snow is shortwave radiation, and this is particularly variable in forested environments (Link and Marks 1999; Hardy et al. 2004; Link et al. 2004). Therefore, it is the purpose of this paper to examine the variability of shortwave irradiance in coniferous forest environments during snowmelt to estimate the significance of this variability to snow-covered area depletion. A companion paper (Essery et al. 2008) focuses on estimating the spatial distribution of shortwave transmission through coniferous canopies using remote sensing and explicit radiative transfer modeling.

2. Variability of shortwave transmission through forest canopies

Forested landscapes have a large spatial distribution of ablation energy because this energy varies according to the structural properties of the canopy [e.g., density, Davis et al. (1997); leaf area index, Pomeroy and Granger (1997)]. Transmittance through canopies with relatively small sky view factors can be estimated using the assumption of isotropic scattering by canopy elements; however, it is generally recognized that there are several features of radiation transmission, extinction, and reflectance that might cause persistent spatial patterns in irradiance to melting snow. These features are strongly controlled by the three-dimensional spatial distribution and the arrangement of forest foliage at both the individual tree and forest stand scales (Anderson 1966; Nilson 1971; Pukkala et al. 1991). These in turn are related to ecological factors such as species composition (Jarvis et al. 1975), productivity (Eagleson 2002), and stage of succession (Ross et al. 1986; Parker et al. 2002). It is possible to link the canopy transmittance of shortwave radiation to laser remote sensing observations of forest structure (Parker et al. 2002). For discontinuous stands, shortwave irradiance into gaps and the north edge of gaps (in the Northern Hemisphere) is much greater than that under more shaded parts of the canopy (Satterlund 1983).

The previously cited literature suggests the following several hypotheses regarding the spatial variability of shortwave irradiance to snow: The first is that the spatial variance will increase with mean irradiance, permitting the calculation of a spatial CV of irradiance (useful in snow-covered area depletion calculations). The second is that the CV will decline with averaging time interval for clear sky conditions. The third is that the variance will be much higher for discontinuous forest stands than for uniform stands.

3. Methods

The main experiments were conducted as part of the National Aeronautics and Space Administration (NASA) Cold Land Processes Experiment (CLPX) in a subalpine lodgepole pine (*Pinus contorta*) forest (39.98°N, 105.98°W; 2780 m above sea level) in the U.S. Forest Service's Fraser Experimental Forest near Fraser, Colorado (Cline et al. 2002). The Fraser Experimental Forest is a long-term research facility of the Rocky Mountain Research Station and has been subject to stand management and snowmelt studies since the 1940s. A relatively uniform lodgepole pine stand and an adjacent discontinuous stand were studied—the same stands were studied by Hardy et al. (2004). The uniform pine site consists of lodgepole pine trees, with an average height of 12.4 m (standard deviation = 2.5 m) and relatively uniform spacing. Trees in the discontinuous site are of mixed species [predominantly lodgepole pine with some Englemann spruce (*Picia engel-*

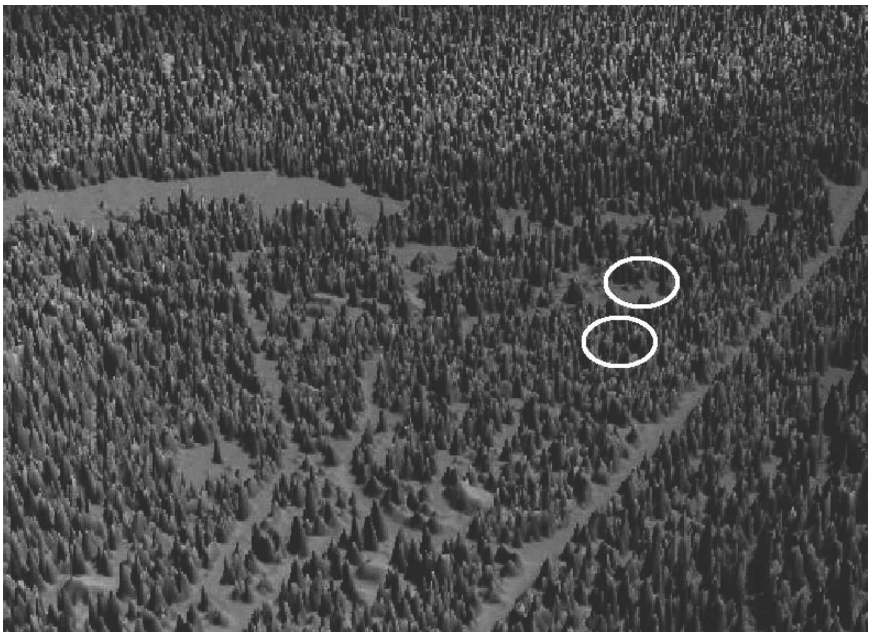

FIG. 1. Rendered representation of the lidar first return of the Fraser pine forest showing the locations of the discontinuous (upper circled area) and uniform (lower circled area) stands.

mannii) and subalpine fir (*Abies lasiocarpa*)], with an average height of 7.8 m (standard deviation = 4.8 m) and heterogeneous spacing.

Arrays of 20 Eppley and Matrix pyranometers were used to measure irradiance. Link et al. (2004) has shown that these arrays are adequate for describing the mean and variability of irradiance in coniferous forests. In the uniform pine site, radiometers were located by selecting a random distance and angle from a central distribution point. In the discontinuous pine site, radiometer placement also considered proximity to tree trucks and placement in canopy gaps. A Kipp and Zonen CM3 pyranometer on a 20-m tower provided above-canopy reference irradiation. Figure 1 shows a rendered image of the lidar first return data with the discontinuous and adjacent uniform forest stands in the Fraser Experimental Forest.

This paper focuses on a 3-day period during the CLPX Intensive Observation Period 2 (IOP 2), 27–29 March 2002 (days 86–88). The snowpack was isothermal and actively melting in this period and had become patchy in the discontinuous pine stand. Weather conditions for the 3 days are summarized in Table 1.

Ancillary data for comparing variability of irradiance and canopy diffuse transmissivity were taken from experiments using radiometer arrays (Link et al. 2004) in the Boreal Ecosystem–Atmosphere Study (BOREAS) in the boreal forest of central Saskatchewan, Canada (Link and Marks 1999), Wolf Creek Research Basin in the montane boreal forest of the Coast Mountains in the southern Yukon Territory (Sicart et al. 2004), and Marmot Creek Research Basin in the montane forests of the Rocky Mountains in southwestern Alberta, Canada (Ellis and Pomeroy 2007). The locations and descriptions of these stands and observations are detailed in Table 2.

TABLE 1. Summary of the weather conditions between days 86 and 88; notice that air temperatures are in the subcanopy at 2 m above the snowpack.

Date	Yearday	Conditions	Min air temperature (°C)	Max air temperature (°C)
27 Mar 2002	86	Overcast No precipitation	−6.8	3.8
28 Mar 2002	87	Clear sky No precipitation	−3.1	6.5
29 Mar 2002	88	Clear sky No precipitation	−7.0	6.2

TABLE 2. Sites where pyranometer array-based measurements of irradiance were available to compare canopy characteristics and the spatial variation of irradiance.

Location	Species	Description	Elev (m)	Lat (°N)	Lon (°W)
Fraser, CO	Lodgepole pine	Uniform	3070	40	105
Fraser, CO	Lodgepole pine	Discontinuous	3070	40	105
Marmot Creek, AB	Lodgepole pine	Uniform	1500	51	115
Candle Lake, SK	Jack pine	Old (BOREAS)	600	54	105
Candle Lake, SK	Black spruce	Old (BOREAS)	400		
Wolf Creek, YT	White spruce	Old, uniform	700	62	135

4. Results

Shortwave variability was first examined by comparing the spatial mean shortwave irradiance above and beneath the canopy at the uniform and discontinuous stands in clear and overcast conditions (Fig. 2). A single pyranometer on a 20-m tower measured above-canopy irradiance, while an array of 20 pyranometers measured mean subcanopy irradiance, with 10 for each forest stand. The above-canopy shortwave irradiance on days 87 and 88 indicated clear sky conditions, dominated by direct-beam radiation. Daily mean transmissivities on these clear days were 0.23 and 0.25 for the uniform stand and 0.52 and 0.56 for the discontinuous stand. On day 86, variable cloud optical depths resulted in substantially reduced irradiance compared to possible direct-beam magnitudes, with the degree of reduction varying considerably during the day. This represented classic overcast sky conditions, dominated by diffuse radiation. Daily mean transmissivities for the overcast day were 0.33 for the uniform stand and 0.56 for the discontinuous stand. It is instructive that there was very little difference in transmissivities for the discontinuous stand between clear and overcast days. However, in the uniform stand, the transmissivity increased 37% on the overcast day compared to the clear days. This is most likely due to the low solar angle at this time of year and the relatively small canopy gap lengths (<2 m) in the uniform canopy; direct-beam radiation would tend to pass through the tree crowns rather than through the gaps for most of the day, whereas diffuse radiation would enter primarily through the gaps. In contrast, the gaps are large (tens of meters) in the discontinuous canopy; therefore, the sun transits the gaps frequently during the day.

5. Analysis

Irradiance is often sampled at short time intervals; snowmelt models run with time intervals from 15 min to days (Gray and Landine 1988; Marks et al. 1999), but snowmelt is a cumulative process over many days. For this reason, irradiance was resampled from minute to day intervals. It was hypothesized that the spatial standard deviation of irradiance would increase with the spatial mean irradiance and that the spatial variation of irradiance to snow would decline with time interval. Figure 3 shows the spatial standard deviation of subcanopy shortwave irradiance for each sampling interval (5 min–24 h) and the corresponding spatial mean shortwave irradiance for both uniform and discontinuous canopies under clear and overcast conditions. Spatial standard deviation and mean were calculated from the 10 pyranometers under each stand for sampling intervals of increasing time length. The sampling intervals were increased by taking longer averages of sampled data; however, longer averages also resulted in smaller sample sizes. In all cases, variability increased with mean irradiance. There was smaller spatial variability of irradiance on the overcast day than on the clear day, and smaller spatial variability of irradiance under the uniform stand than under the discontinuous stand. On the overcast day, there was a linear relationship between spatial standard deviation and mean for small irradiances. In contrast, the rate of change of standard deviation for larger values of irradiance increased with increasing mean, causing an overall nonlinear relation-

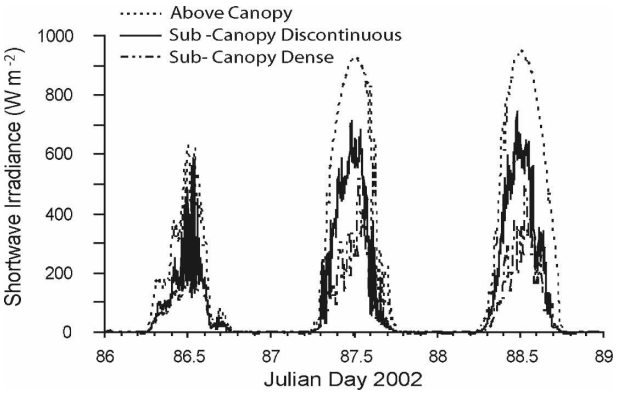

FIG. 2. Shortwave irradiance measured above canopy and mean irradiance from 10 pyranometers under each discontinuous and uniform pine canopy.

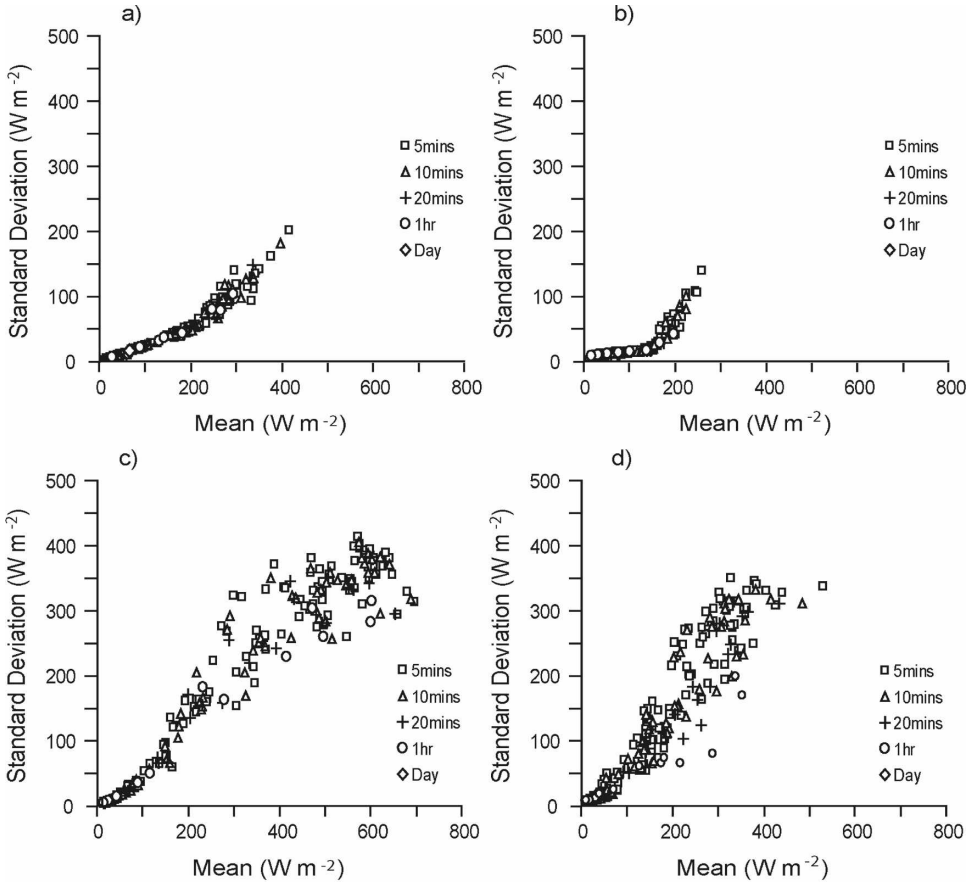

FIG. 3. Standard deviation and mean of shortwave subcanopy irradiance for various sampling time intervals (5 min–1 day) under (a), (c) discontinuous and (b), (d) uniform canopy for (a), (b) overcast (day 86) and (c), (d) clear (day 87) conditions. Day 88 (not shown) was similar to day 87.

ship. This effect was most pronounced under the uniform stand. On the clear day, the standard deviation increased linearly with the mean until high values ($\sim$400 W m^{-2}) were reached, at which point the rate of change began to decrease. Again, an overall nonlinear relationship was observed, but a concave instead of a convex pattern developed at higher radiation values. The effect of increasing the sampling interval was a decrease in the mean and standard deviation along the established uniform and discontinuous canopy relationships on the overcast day. However, as the sampling interval increased, there was a larger decrease in the standard deviation on the clear day than there was in the mean.

The spatial CV of shortwave radiation, the ratio of standard deviation to the mean, is the slope of the points shown in Fig. 3. The linear relationships between spatial standard deviation and the mean for part of their range (Fig. 3) suggest that the CVs can be evaluated as a function of sampling interval for both stands and sky conditions. The slope between spatial standard deviation (Y) and mean (X), forcing an intercept of zero, was used to estimate the CVs for each day of observations. The CVs were calculated for the full range of intervals from 1 min to 1 day. The R^2 values for these linear regressions varied from 0.91–0.97 for the discontinuous canopy to 0.87–0.95 for the uniform canopy on clear days, with lower R^2 values of 0.63–0.85 for the uniform canopy on the overcast day. An analysis of variance of the regressions showed F statistics for all linear fits that were statistically significant, with a probability of 0.95 or better. The fit of the relationships generally improved with longer sampling intervals. The spatial CV for daily irradiance was calculated directly (the daily standard deviation divided by the daily mean).

Figure 4 shows the change in the spatial CV with temporal sampling interval. Whereas meaningful tests of statistical significance cannot be conducted on just a few values that result from linear regressions, the strong decrease in CV with sampling interval is unambiguous for clear conditions (51%–88%) and for the

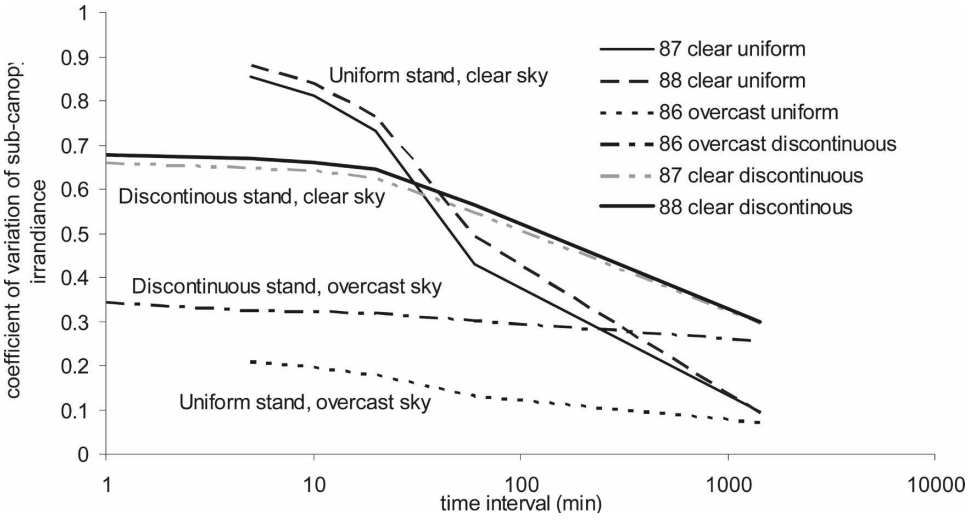

FIG. 4. CV of subcanopy irradiance for uniform and discontinuous stands on clear (days 87 and 88) and overcast (day 86) days as a function of sampling time intervals (1 min–1 day).

uniform stand in cloudy conditions (66%); the mild decline for the discontinuous stand in cloudy conditions (20%) is relatively unimportant. These differing rates of change resulted in the ratio of discontinuous to uniform stand CV on overcast days rising from ~1.75 to ~3, as the sampling interval increased to daily periods. The CV under clear skies showed very complex behavior and a rapid drop with an increasing sampling interval. The CVs dropped from values approximately 2–4 times higher than those for overcast skies at short sampling intervals to values that approximately equaled the overcast values at daily sampling intervals. The ratio of uniform to discontinuous stand spatial CV dropped from 1.3 to 0.3 as the sampling interval increased to daily periods. This caused the most spatially variable canopy to switch from uniform to discontinuous as the sampling interval increased. The fundamental result is that for daily time intervals, it is difficult to distinguish the CV of irradiance from clear and cloudy days; the spatial CV is much more influenced by the canopy structure than by sky condition. These results are consistent with radiative transfer modeling results for the same canopies presented in a companion paper (Essery et al. 2008).

At short sampling intervals, the large difference between the CV for clear and overcast days is likely due to the contribution to variability by small-scale transmittance through gaps and branch and needle scattering of direct-beam radiation. As described by Roujean (1999), scattering by branches and needles causes complex shadows and "speckled light" to move across the pyranometers on the time scale of minutes. This effect would be most prevalent where the canopy is most prevalent—the uniform stand. The low magnitude of the CV on overcast days and daily sampling intervals was due to the variability in these conditions being sustained only by canopy gap structure and its effect on the sky view factor (Hardy et al. 2004). The effect of branches and needles would be undetectable either for daily average irradiance or when irradiation is dominated by diffuse radiation. On daily intervals or overcast days, the CV was higher in the discontinuous canopy where large canopy gaps induced persistent spatial patterns of irradiance. On overcast days or daily intervals, only the canopy properties (likely gap structure) influenced the variability of shortwave irradiance. The essential information for snowmelt modeling is that for daily time intervals, cloudiness had, at best, a very small effect on the spatial variability of shortwave irradiance; however, cloudiness must be taken into account for hourly time intervals or less where the spatial variability can either double (discontinuous stand) or triple (uniform stand) from overcast values as skies become clear. Because snowmelt models accumulate melt, cloudiness will not affect the spatial CV of irradiance during the main melt period, regardless of the short calculation intervals of some melt models.

6. Extrapolation and discussion

The CLPX results suggested that the variability of irradiance is influenced by canopy structure. To see if the CV of subcanopy irradiance could be described by a canopy structure parameter, the CV for the two Fraser stands and from similar radiometer array observations in other canopies were examined. Data were

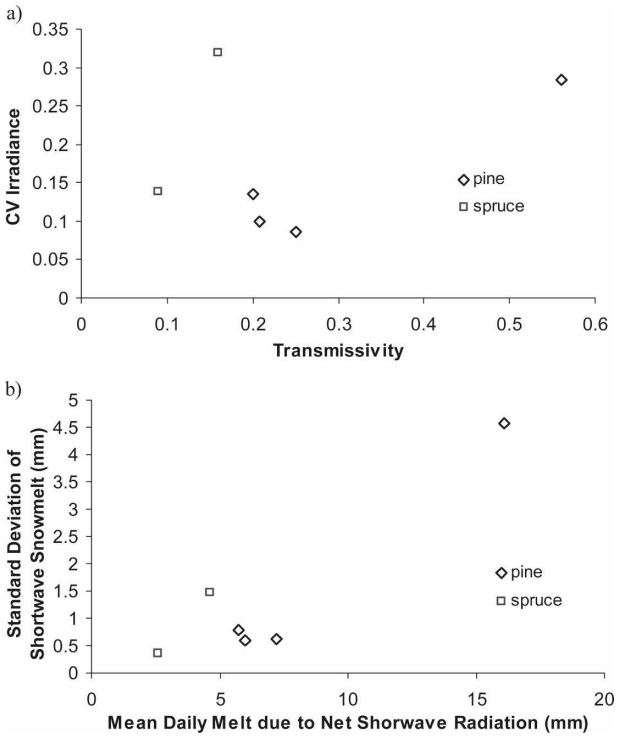

FIG. 5. (a) Coefficient of variation of irradiance vs transmissivity for overcast days (diffuse transmissivity) for pine (Fraser, CO; BOREAS sites, central SK; Marmot Creek, AB) and spruce canopies (BOREAS sites, central SK; Wolf Creek, YT). (b) Standard deviation vs mean daily snowmelt energy expressed in units of SWE depth (mm) resulting from net subcanopy shortwave radiation.

obtained from experiments with compatible methodologies in a mature jack pine stand in the BOREAS experiment (near Candle Lake, Saskatchewan, Canada), a mature uniform lodgepole pine stand in Marmot Creek Research Basin (Kananaskis Country, Alberta, Canada), an old black spruce stand in the BOREAS experiment, and a mature white spruce stand in Wolf Creek Research Basin (near Whitehorse, Yukon Territory, Canada). The CVs for these canopies are plotted against overcast day transmissivity in Fig. 5a. The overcast day transmissivity is due to diffuse radiation and is therefore approximately equal to the sky view fraction and to one-canopy closure; thus, it is a readily available forest parameter, and it was measured at each site in the same way. The three uniform pine stands (Fraser uniform, Marmot, and BOREAS mature jack pine) all cluster with the CV from 0.08 to 0.14 and with transmissivity from 0.20 to 0.25. The white spruce stand at Wolf Creek also has a CV of 0.14 but a lower corresponding transmissivity. The discontinuous pine stand (Fraser) has a CV and transmissivity that both are ~2.8 times higher than for the uniform pine stands. The old black spruce stand (BOREAS) also has a high CV (0.31) but a much lower corresponding transmissivity than the Fraser pine. The scaling of the CV with transmissivity for pine is encouraging but insufficient to determine a reliable relationship. The two spruce stands have a high CV for relatively small values of transmissivity. The difference between spruce and pine may be due to differences in tree growth forms. Spruce canopies are more clumped than pine, the tapered form of the spruce has larger gaps than a pine for the same sky view fraction. It was hypothesized that when sky view exceeds canopy coverage (transmissivity >0.5), variability should then begin to drop with increasing sky view fraction. Unfortunately, this dataset is not sufficient to confidently describe the relationship between the variability of irradiance and sky view fraction.

To calculate the variability of irradiance in terms of snowmelt energy, a daily insolation of 12 MJ day^{-1} was assumed (typical of bright sky conditions for March in Colorado, April in southern Canada, and May in northern Canada) and a subcanopy albedo of 0.8 was chosen (Hardy et al. 2000). Transmissivity values were used to convert insolation to subcanopy irradiance, and irradiance was multiplied by the albedo to produce subcanopy net shortwave energy. Figure 5b shows the standard deviation of daily melt energy (mm day^{-1}) versus the mean daily melt energy (mm day^{-1}), in which melt energy is due to net shortwave radiation. Because high transmissivities are associated with both higher subcanopy irradiance and higher variation of irradiance, there is less difference between pine and spruce stands, and a linear increase between standard deviation and mean daily melt energy is apparent (an analysis of variance F test of the regression shows this to be significant, with a 99% level of confidence), with a standard error of 0.68 mm day^{-1}. This means the greater the discontinuity, the greater the irradiance and variance of irradiance, which stabilizes the CV of melt energy from shortwave irradiance. The best fit CV of melt energy resulting from net shortwave radiation is 0.23, with an R^2 of 0.77. This relatively stable CV provides a provisional value that can be used for estimating the daily variability of melt energy from shortwave radiation under conifer stands at mid to high latitudes under clear or overcast skies; however, a larger observational dataset to confirm its stability is needed.

To test whether a CV of melt energy of this magnitude can have a significant impact on the shape of a snow cover depletion curve, a synthetic melt simulation was created using a grid of 110 cells with a uniform initial snowpack of 50 mm SWE and a normal distribution of melt energy having a mean of 5-mm melt per

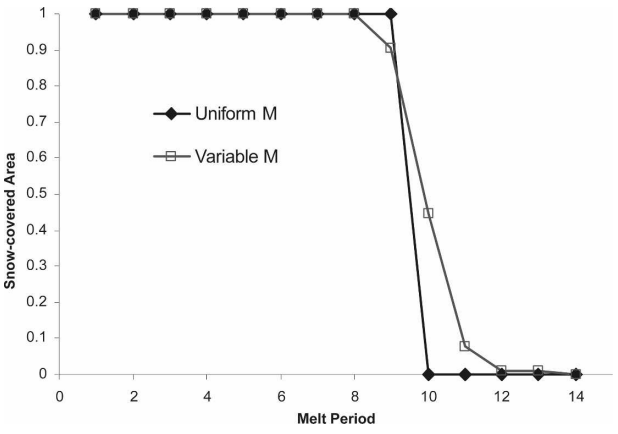

FIG. 6. Modeled depletion of snow-covered area from a 50-mm SWE uniform snow cover with a mean 5 mm of melt energy applied each period—a uniform melt and a variable melt with a spatial CV of 2.3.

period with a spatial CV of 0.23. The simulation was run for 14 periods, with a different normal distribution of melt energy applied each period. The fractional snow cover f_s was calculated as the number of cells having SWE > 0. Another simulation was run with the same initial SWE but with constant melt energy of 5 mm per period applied to all cells. Figure 6 shows the two simulations of the snow-covered area. The simulation with constant melt energy drops from $f_s = 1$ to 0 after 10 melt periods. This immediate transition from snow covered to snow free is unrealistically fast. The simulation with a distribution of melt energy showed a smoother decline in f_s, with time and an areal melt duration extended by two periods (20%). Hence, the effect of including distributed melt energy by the variation resulting from shortwave irradiance in forests extends the duration of snowmelt, which consequently must reduce peak melt rates. It should be noted that this simulation assumes a constant SWE over the snowfield, which is unrealistic. If there were also a frequency distribution of initial SWE and if the melt energy were negatively correlated with SWE then this effect could be enhanced substantially (Pomeroy et al. 2001; Essery and Pomeroy 2004).

7. Conclusions

The spatial variation of shortwave irradiance to snow can affect the depletion of the snow-covered area and areal melt rates, but the magnitude of this variation has not been quantified by field measurements during melt. The spatial standard deviation of subcanopy irradiance under a mountain pine canopy was found to scale with the spatial mean irradiance, permitting the estimation of the spatial coefficient of variation of subcanopy irradiance (CV). The spatial CV decreased with increasing irradiance averaging interval, showing the sharpest declines under clear sky conditions and for relatively uniform stands. At daily averaging intervals, there was little influence of cloudiness on the CV, and the CV for the uniform stand was much lower than that for the discontinuous stand. The CV for daily intervals was compared to the mean diffuse transmissivity of the canopy for several mountain and boreal coniferous forests, and differences resulting from canopy type and transmissivity were noted. However, there was insufficient data and too much scatter in the relationships to relate the CV to canopy structure. The spatial CV of melt energy resulting from net subcanopy shortwave radiation was provisionally estimated as 0.23 from this dataset, for all sky conditions and canopy types. Applying this CV in a snow-covered area depletion calculation increased the snow-covered period by 20%, compared to a simulation with spatially constant melt energy. Knowledge of this variability in melt energy will help in estimating snow cover depletion rates during snowmelt under forest canopies using models that continue from that proposed by Essery and Pomeroy (2004).

Acknowledgments. The financial support of the NOAA GEWEX Americas Prediction Project (GAPP), U.S. Army Corps of Engineers, Cold Regions Research and Engineering Laboratory, USDA Agricultural Research Service, Canadian Foundation for Climate and Atmospheric Sciences, and the Natural Sciences and Engineering Research Council of Canada is greatly appreciated. The authors thank three anonymous reviewers and the guest editor for comments that improved this manuscript.

REFERENCES

Anderson, M. C., 1966: Stand structure and light penetration. II. A theoretical analysis. *J. Appl. Ecol.,* **3,** 41–54.

Brubaker, K. L., and M. Menoes, 2001: A technique to estimate snow depletion curves from time-series data using the beta distribution. *Proc. 58th Annual Eastern Snow Conf.,* Ottawa, ON, Canada, ESC and Canadian Geophysical Union, 343–346.

Buttle, J. M., and J. J. McDonnell, 1987: Modelling the areal depletion of snowcover in a forested catchment. *J. Hydrol.,* **90,** 43–60.

Cline, D., and Coauthors, 2002: Overview of the NASA cold land processes field experiment (CLPX-2002). *Microwave Remote Sensing of the Atmosphere and Environment III,* C. D. Kummerow, J. Jiang, and S. Uratuka, Eds., International Society for Optical Engineering (SPIE Proceedings, Vol. 4894), 361–372.

Davis, R. E., J. P. Hardy, W. Ni, C. Woodcock, J. C. McKenzie, R.

Jordan, and X. Li, 1997: Variation of snow cover ablation in the boreal forest: A sensitivity study on the effects of conifer canopy. *J. Geophys. Res.,* **102,** 29 389–29 395.

Donald, J. R., E. D. Soulis, N. Kouwen, and A. Pietroniro, 1995: A land cover-based snow cover representation for distributed hydrological models. *Water Resour. Res.,* **31,** 995–1009.

Eagleson, P. S., 2002: *Ecohydrology: Darwinian Expression of Vegetation Form and Function*. Cambridge University Press, 443 pp.

Ellis, C. R., and J. W. Pomeroy, 2007: Estimating sub-canopy shortwave irradiance to melting snow on forested slopes. *Hydrol. Processes,* **21,** 2581–2593.

Essery, R. L. H., and J. W. Pomeroy, 2004: Implications of spatial distributions of snow mass and melt rate for snow-cover depletion: Theoretical considerations. *Ann. Glaciol.,* **38,** 261–265.

——, and Coauthors, 2008: Radiative transfer modeling of a coniferous canopy characterized by airborne remote sensing. *J. Hydrometeor.,* **9,** 228–241.

Faria, D. A., J. W. Pomeroy, and R. L. H. Essery, 2000: Effect of covariance between ablation and snow water equivalent on depletion of snow-covered area in a forest. *Hydrol. Processes,* **14,** 2683–2695.

Gray, D. M., and P. G. Landine, 1988: An energy-budget snowmelt model for the Canadian Prairies. *Can. J. Earth Sci.,* **25,** 1292–1303.

Hardy, J. P., R. A. Melloh, P. Robinson, and R. Jordan, 2000: Incorporating effects of forest litter in a snow process model. *Hydrol. Processes,* **14,** 3227–3237.

——, ——, G. Koenig, D. Marks, A. Winstral, J. W. Pomeroy, and T. Link, 2004: Solar radiation transmission through conifer canopies. *Agric. For. Meteor.,* **126,** 257–270.

Jarvis, P. G., G. B. James, and J. J. Landsberg, 1975: Coniferous forest. *Case Studies,* J. L. Monteith, Ed., Vol. 2, *Vegetation and the Atmosphere,* Academic Press, 171–240 pp.

Link, T. E., and D. Marks, 1999: Point simulation of seasonal snow cover dynamics beneath boreal forest canopies. *J. Geophys. Res.,* **104,** 841–858.

——, J. P. Hardy, and D. Marks, 2004: A deterministic method to characterize canopy radiative transfer properties. *Hydrol. Processes,* **18,** 3583–3594.

Marks, D., and A. Winstral, 2001: Comparison of snow deposition, the snow cover energy balance, and snowmelt at two sites in a semiarid mountain basin. *J. Hydrometeor.,* **2,** 213–227.

——, J. Domingo, D. Susong, T. Link, and D. Garen, 1999: A spatially distributed energy balance snowmelt model for application in mountain basins. *Hydrol. Processes,* **13,** 1935–1959.

Nilson, T. A., 1971: A theoretical analysis of the frequency of gaps in plant stands. *Agric. For. Meteor.,* **8,** 25–38.

Parker, G. G., M. Davis, and S. Moon Chapotin, 2002: Canopy light transmittance in Douglas-fir–western hemlock stands. *Tree Physiol.,* **22,** 147–157.

Pomeroy, J. W., and R. J. Granger, 1997: Sustainability of the western Canadian boreal forest under changing hydrological conditions. I. Snow accumulation and ablation. *Proc. Sustainability of Water Resources under Increasing Uncertainty Symp.,* Rabat, Morocco, Int. Commission on Water Resource Systems and Cosponors, IAHS Publication 240, 237–242.

——, D. M. Gray, K. R. Shook, B. Toth, R. L. H. Essery, A. Pietroniro, and N. Hedstrom, 1998: An evaluation of snow accumulation and ablation processes for land surface modelling. *Hydrol. Processes,* **12,** 2339–2367.

——, S. Hanson, and D. A. Faria, 2001: Small-scale variation in snowmelt energy in a boreal forest: An additional factor controlling depletion of snow cover? *Proc. 58th Annual Eastern Snow Conf.,* Ottawa, ON, Canada, ESC and Canadian Geophysical Union, 85–96.

——, R. L. H. Essery, and B. Toth, 2004: Implications of spatial distributions of snow mass and melt rate on snow-cover depletion: Observations in a subarctic mountain catchment. *Ann. Glaciol.,* **38,** 195–201.

Pukkala, T., T. Becker, T. Kuuluvainen, and P. Oker-Blom, 1991: Predicting spatial distribution of direct radiation below forest canopies. *Agric. For. Meteor.,* **55,** 295–307.

Ross, M. S., L. B. Flanagan, and G. H. La Roi, 1986: Seasonal and successional changes in light quality and quantity in the understory of boreal forest ecosystems. *Can. J. Bot.,* **64,** 2792–2799.

Roujean, J.-L., 1999: Measurements of PAR transmittance within boreal forest stands during BOREAS. *Agric. For. Meteor.,* **93,** 1–6.

Satterlund, D. R., 1983: Forest shadows: How much shelter in a shelterwood? *For. Ecol. Manage.,* **5,** 23–37.

Shook, K., 1995: Simulation of the ablation of prairie snowcovers. Ph.D. thesis, University of Saskatchewan, 189 pp.

——, J. W. Pomeroy, and D. M. Gray, 1993: Temporal variation in snow-covered area during melt in Prairie and Alpine environments. *Nord. Hydrol.,* **24,** 183–198.

Sicart, J. E., J. W. Pomeroy, R. L. H. Essery, J. E. Hardy, T. Link, and D. Marks, 2004: A sensitivity study of daytime net radiation during snowmelt to forest canopy and atmospheric conditions. *J. Hydrometeor.,* **5,** 774–784.